A&A 495, 195–199 (2009)
DOI: 10.1051/0004-6361:200810467

Astronomy & Astrophysics

Hα spectropolarimetry of RY Tauri and PX Vulpeculae⋆ *(Research Note)*

A. Pereyra[1], A. M. Magalhães[2], and F. X. de Araújo[1]

[1] Observatório Nacional, Rua General José Cristino 77, São Cristovão, 20921-400 Rio de Janeiro, Brazil
e-mail: pereyra@on.br
[2] Departamento de Astronomia, IAG, Universidade de São Paulo, Rua do Matão 1226, São Paulo, SP 05508-900, Brazil

Received 25 June 2008 / Accepted 17 November 2008

ABSTRACT

Aims. To detect line effects using spectropolarimetry in order to find evidence of rotating disks and their respective symmetry axes in T Tauri stars.
Methods. We used the IAGPOL imaging polarimeter along with the Eucalyptus-IFU to obtain spectropolarimetric measurements of the T Tauri stars RY Tau (two epochs) and PX Vul (one epoch). Evidence of line effects showing a loop in the $Q-U$ diagram favors a compact rather than an extended source for the line photons in a rotating disk. In addition, the polarization position angle (PA) obtained using the line effect can constrain the symmetry axis of the disk.
Results. RY Tau shows a variable Hα double peak in 2004–2005 data. A polarization line effect is evident in the $Q-U$ diagram for both epochs confirming a clockwise rotating disk. A single loop is evident in 2004 changing to a linear excursion plus a loop in 2005. Interestingly, the intrinsic PA calculated using the line effect is consistent between our two epochs (∼167°). An alternative intrinsic PA computed from the interstellar polarization-corrected continuum and averaged between 2001–2005 yielded a PA ∼ 137°. This last value is closer to perpendicular to the observed disk direction (∼25°), as expected from single scattering in an optically thin disk. For PX Vul, we detected spectral variability in Hα along with non-variable continuum polarization when compared with previous data. The $Q-U$ diagram shows a well-defined loop in Hα associated with a counter-clockwise rotating disk. The symmetry axis inferred from the line effect has a PA ∼ 91° (with an ambiguity of 90°). Our results confirm previous evidence that the emission line in T Tauri stars has its origin in a compact source scattered off a rotating accretion disk.

Key words. polarization – stars: individual: RY Tau – stars: individual: PX Vul – stars: circumstellar matter

1. Introduction

Over the last years spectropolarimetry has become a powerful tool for studying envelopes (or disks) around unresolved young stellar objects (YSOs). In this context, the analysis of the Stokes parameters $Q-U$ diagram has become to be a fundamental diagnostic tool for polarization line detections (Oudmaijer & Drew 1999; Vink et al. 2002, 2003 – hereinafter V03, 2005a).

Considering the line effects, the most simple case happens when the emission lines are formed over a much larger volume than continuum. In this case, the circumstellar scattering material will polarize the continuum light more than the line photons. These will add mainly unpolarized flux because they will be less scattered, and therefore the net polarization across the emission line will be reduced. This feature is usually called the depolarization line effect (Clarke & McLean 1974) and a linear excursion is expected in the $Q-U$ diagram with the position angle (PA) unchanged.

Models to explain the line effect including rotation also have been explored (Poeckert & Marlborough 1977; Wood et al. 1993; Vink et al. 2005b). If the line photons originate from a compact source, the polarization pattern will depend on the specific geometry and bulk motions of the scattering particles surrounding the compact line source. In a rotating disk-like configuration, the subsequent breaking of left-right reflection symmetry in the velocity fields leads to a change in polarization angle with wavelength, which appears as a loop in the $Q-U$ diagram (Vink et al. 2002). Interestingly, the sense of rotation of the envelope/disk as seen from the Earth also can be retrieved from the direction in which the PA rotates around the loop in the $Q-U$ diagram (Poeckert & Marlborough 1977).

The survey of Vink et al. (2005a) found that most (9/10) of the T Tauri stars (TTS) shown line effects associated with a compact source of line photons that is scattered off a rotating accretion disk. This means that loops on the $Q-U$ diagram must be a well-defined signature for TTS. The statistics clearly have to be increased to confirm this issue.

In this work, we report spectropolarimetric observations around Hα of the TTS RY Tau and PX Vul. These are the first results of an ongoing spectropolarimetric survey of YSOs. The observations and data reduction are presented in Sect. 2. The results are shown in Sect. 3. A summary with the final conclusions are drawn in Sect. 4.

2. Observations

The observations were made in two runs in 2004 and 2005 using the 1.6 m telescope at the Observatório do Pico dos Dias (OPD), Brazil. We used IAGPOL, the IAG imaging polarimeter (Magalhães et al. 1996; Pereyra 2000), along with Eucalyptus-IFU (EIFU, de Oliveira et al. 2003). EIFU is an integral field unit composed of an array of 32 × 16 50 μm fibers that covers a field of 30″ × 15″ on the sky with a scale of 0.93″ per pixel (Fig. 1, left). The detector used was a Marconi 2048 × 4608 pixel

⋆ Based on observations obtained at the *Observatório do Pico dos Dias*, LNA/MCT, Itajubá, Brazil.

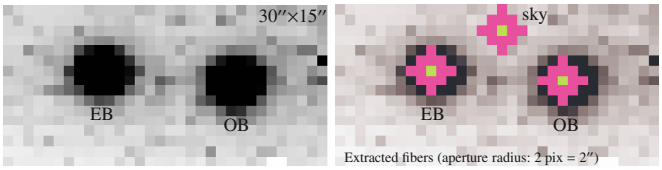

Fig. 1. *Left*: 2-D reconstructed image from EIFU+IAGPOL showing the ordinary (OB) and extraordinary (EB) beams for point sources in one of the waveplate positions. The field size is 30″ × 15″ with an scale of 0.93″ per pixel. *Right*: extracted fibers (in magenta) used to construct the ord., ext. and sky spectra in each waveplate position for an appropriate aperture radius. In this example, $r = 2$ pix or 13 stacked fibers. The central fiber is shown in green for each spectra.

back-illuminated CCD with 13.5 μm^2 per pixel. The spectral range used for EIFU was ~600 Å centered at Hα (R = 4000) that yields a resolution of ~0.3 Å per pixel.

We used IAGPOL in linear polarization mode with a Savart plate as an analyzer and an achromatic $\lambda/2$-waveplate as a retarder. Each measurement consisted of four or eight waveplate positions separated by 22.°5. The IAGPOL+EIFU setup permits that the beam collected by the telescope and divided in two orthogonal polarization beams by IAGPOL will be projected on the EIFU fiber array. Then, spectropolarimetry can be done using the ordinary and extraordinary beams that yield the -o and -e spectra in each waveplate position. A log of observations is shown in Table 1.

We used standard *IRAF*[1] procedures for IFU reductions in each waveplate position image including bias and flatfielding corrections along with wavelength calibrations. Then, a special routine was developed to extract and stack fibers for the -o and -e beams and the sky region (Fig. 1, right). The optimum aperture radius for the fibers extraction was selected by minimizing the polarimetric errors. Therefore, three spectra were constructed at each waveplate position: O(λ), E(λ) and sky(λ) where special care was taken to remove cosmic rays. The sky spectrum was constructed stacking fibers away from the -o and -e beams (Fig. 1, right). Then, the sky was subtracted of the -o and -e spectra in each waveplate position image. Several relative positions for the sky were tested with similar results. After that, we used the SPECPOL[2] package to construct the flux, polarization, polarization PA and polarized flux spectra for a proper binning. This package allows binning of the spectra using a variable bin size set by a selected and constant polarization error per bin. The errors are obtained from the residuals of the observations at each waveplate position image with respect to the expected cosine curve. In general, they are consistent with the photon statistics.

Observations of polarized standard stars in each run yielded the position angle correction to the equatorial system (PA$_{corr}$) and permitted us to check the polarization efficiency of our setup. Our measurements are in agreement with the literature values within one sigma. In addition, the instrumental polarization was checked using unpolarized stars and estimated to be lower than 0.2%, and therefore no correction was needed. A summary of the calibration data is shown in Table 2. Typical signal-to-noise ratios (per bin) gathered by our setup for the sources in this work are between 170 and 250. We checked for the polarization bias effect and it is shown to be negligible.

[1] *IRAF* is distributed by the National Optical Astronomy Observatory, which is operated by the Association of Universities for Research in Astronomy, Inc., under cooperative agreement with the National Science Foundation.

[2] The original version of SPECPOL was written by A. Carciofi.

Table 1. Log of observations.

Object	V^a (mag)	Date	N^b	Total IT^c (s)
		T Tauri		
RY Tau	10.2	2004/Sep./05	8	2400
		2005/Sep./03	4	2400
PX Vul	11.7	2005/Sep./03	8	4800
		standards		
HD 147084^d	4.6	2004/Sep./05	8	1600
HD 187929^d	3.9	2005/Sep./03	8	640
HD 10476^e	5.2	2005/Sep./03	8	800

[a] From Simbad; [b] number of waveplate positions; [c] total integration time (N × individual IT by waveplate position); [d] polarized; [e] unpolarized.

Table 2. Calibration summary.

Object	P_{obs}[a] (%)	PA$_{obs}$[a] (°)	P_{lit}[b] (%)	PA$_{lit}$[b] (°)	PA$_{corr}$ (°)
HD 147084	4.5 (0.2)	0.2	4.50 (0.01)	33.2	+33.0
HD 187929	1.5 (0.2)	37.9	1.62 (0.05)	91.0	+53.1
HD 10476	0.2 (0.2)	–	0.02 (0.01)	–	–

Errors in parenthesis. [a] Mean values for a spectrum binned with a polarization error (per bin) of 0.2%, except HD 10476 (unbinned). The quoted polarization error is the average error per bin. [b] References: HD 147084, Tapia (1988), *R* filter; HD 187929, Bailey & Hough (1982), *R* filter; HD 10476, Bastien et al. (1988), *V* filter.

3. Results

3.1. RY Tau

RY Tau is a classical TTS (F8III type, Mora et al. 2001) with a high optical variability and possibly associated with variable circumstellar obscuration as occurs in UX Ori type stars (Beck & Simon 2001). Spectral variability also has been observed (Vrba et al. 1993; Petrov et al. 1999) without a clear correlation between the Hα line strength and the optical magnitudes.

RY Tau shows a historical strong linear polarization variability (Hough et al. 1981; Bastien 1982; Bergner et al. 1987, V03 and references therein). The proposed polarizing mechanisms include rotational modulations by cool and hot spots on the stellar surface (Stassun & Wood 1999) and variable extinction by a dusty disk (Ménard & Bastien 1992). Recently, robust evidence of a bipolar jet (PA$_{jet}$ = 115°) was found in RY Tau (St-Onge & Bastien 2008) using Hα-continuum imaging that can be used to infer the direction of the unresolved disk and constrain the polarimetric information.

Table 3 shows the observed continuum polarization for RY Tau integrated along the full range of our spectra. A slight enhancement of the continuum polarization level is observed with the PA practically unchanged (~14°) in one year. Our values are comparable with the data from Vink et al. (2005a) between 2001 and 2003. The spectropolarimetry around Hα is indicated in Fig. 2. The spectral range of the top spectra is only of 45 Å for a better visualization of the line feature. The spectra are binned using a variable bin size with a constant polarization error (per bin) of 0.3% and 0.15% for the 2004 and 2005[3] data, respectively. These errors are the best compromise between

[3] The Stokes parameter solution with few waveplate positions (as in the 2005 data) tends to underestimate the polarization error (per bin). In order to detect the line effect, the 2005 data was rebinned at a level that guaranteed the best compromise between the line effect detection and the minimum dispersion of the continuum polarization.

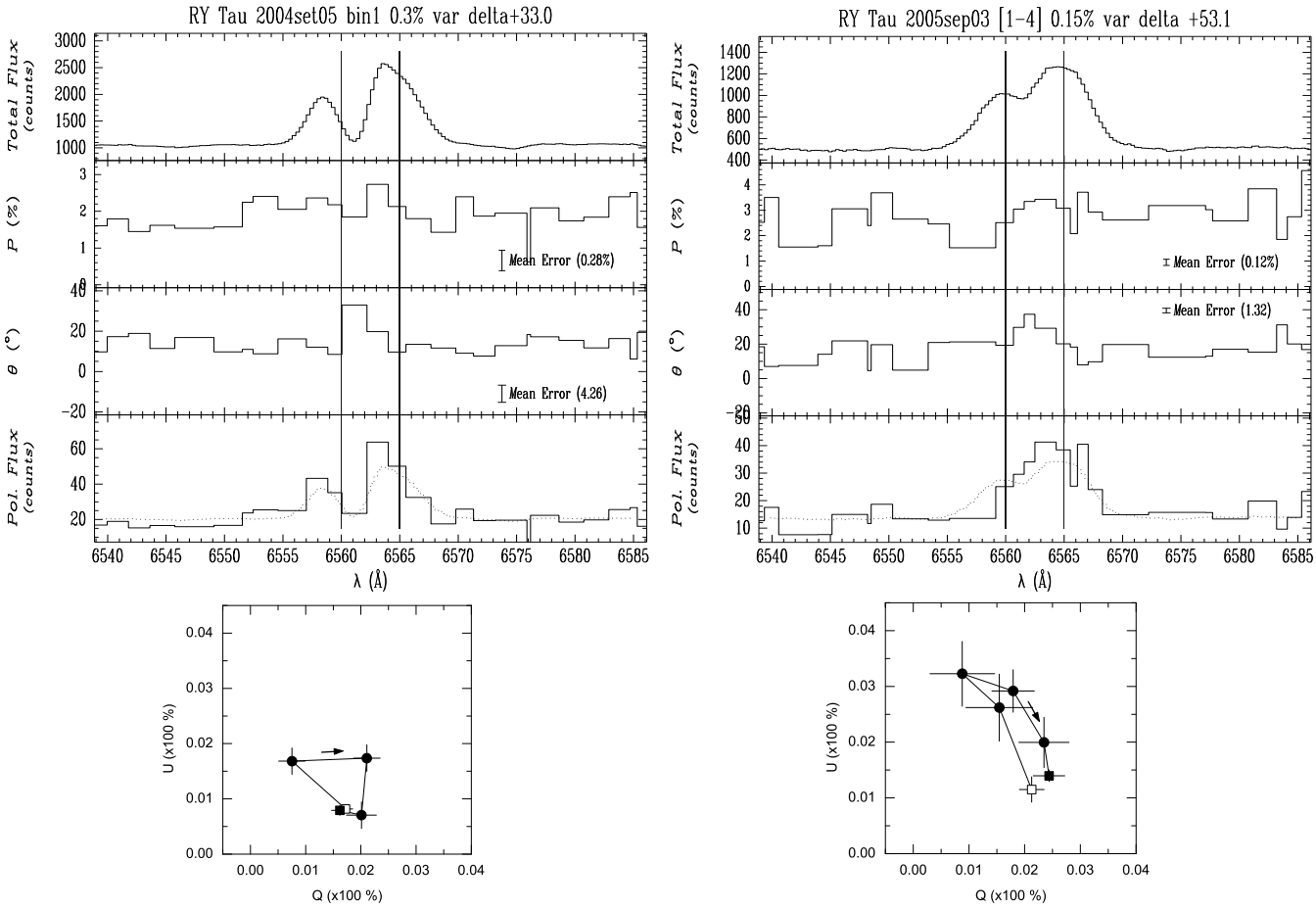

Fig. 2. Spectropolarimetry of RY Tau around Hα on 2004/Sep./05 (*left*) and 2005/Sep./03 (*right*). *Top*: the vertical lines indicate the region (6560−6565 Å) where the line effect is evident. The spectra show the total flux (*top*), polarization (*upper middle*), polarization PA (*lower middle*), and polarization flux (*bottom*) binned using a variable bin size with a constant polarization error (per bin) of 0.3% and 0.15% for the 2004 and 2005 data, respectively. *Bottom*: $Q-U$ diagram showing the line effect (black dots). The direction in which the wavelength increases is also indicated (arrow) along with the mean values for the blue (white square) and red (black square) continuum. The errors plotted around the line effect assume photon statistics directly.

Table 3. Results.

Object	Date	P_{obs}[a] (%)	PA_{obs}[a] (°)	PA_{int} (°)
RY Tau	2004/Sep./05	1.8 (0.3)	11 (5)	171 (11)
	2005/Sep./03	2.6 (0.2)	16 (2)	161[b] (4)
PX Vul	2005/Sep./03	3.2 (0.3)	33 (2)	91[c] (25)

Errors in parenthesis. [a] Mean values for a spectrum binned with a polarization error (per bin) of 0.3%. The quoted polarization error is the averaged error per bin. [b] Rebinned at 0.15% per bin. [c] Or 91+90.

a minimum error (per bin) and line effect detection. The lower plots are the $Q-U$ diagrams showing the line effect.

In 2004, the total flux of Hα appeared as a double-peaked profile with the central dip at the continuum level and the redder peak more intense. On the other hand, the 2005 data again shown a similar double-peak but with the central dip just below the blue peak. The AVVSO database (Henden 2007) shows that RY Tau on average faded from $V \sim 10.0$ mag on 2004/Sep. to ∼10.8 mag on 2005/Sep. The relative intensities of the Hα emission components remained practically constant between the two epochs and can be classified as II−B type (Reipurth, Pedrosa & Lago 1996). We did not find evidence of an increment of Hα when the star is dimmed (Petrov et al. 1999).

We detected the Hα polarization line effect for RY Tau using the $Q-U$ diagrams (Fig. 2, bottom) around the central dip (between 6560−6565 Å). This wavelength range is also indicated in each spectrum (Fig. 2, top) for a better comparison. In 2004, the line effect produces a loop as already reported by V03. Nevertheless, the 2005 data show a stronger and more complex pattern that resembles a mix between a loop and a linear excursion. The integrated continuum polarization immediately before and after the line effect is the same in each epoch. Interestingly, the direction in which the wavelength increases around the loop (indicated by the arrow) has the same sense in our two epochs (and also in V03). Therefore, this confirms that the disk of RY Tau rotates in a clockwise direction as seen by an observer on the Earth.

In order to determine the intrinsic PA (PA_{int}) we used a linear fit of the points that display the line effect in the $Q-U$ diagram. Formally, the slope of the fit yields two possible solutions (PA_{int} and $PA_{int} + 90°$). In general, this ambiguity is solved by the solution more consistent with the relative positions of the interstellar polarization (ISP) and the observed polarization in the $Q-U$ diagram (Schulte-Ladbeck et al. 1994).

Figure 3 shows the observed continuum polarization and the PA_{int} directions obtained from the line effect for our two epochs (Table 3). The ISP toward RY Tau (2.8% at PA = 26°)

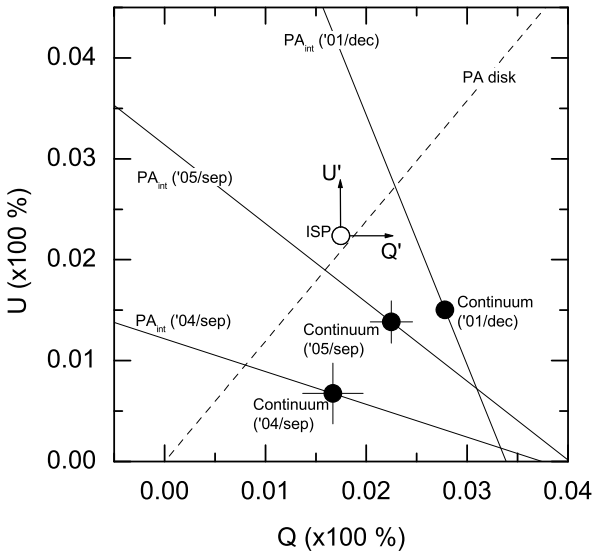

Fig. 3. $Q-U$ diagram for RY Tau showing the intrinsic polarization PA (solid lines) from the Hα line effect in three epochs (2001/Dec. from Vink et al. 2003; and, 2004/Sep. and 2005/Sep. from this work). The continuum polarization around Hα also is shown in each case (black dots). The interstellar polarization (Petrov et al. 1999) is also indicated (white dot) along with the PA disk (dashed line, St-Onge & Bastien 2008). The arrows indicate the reference system (Q',U') corrected for the ISP.

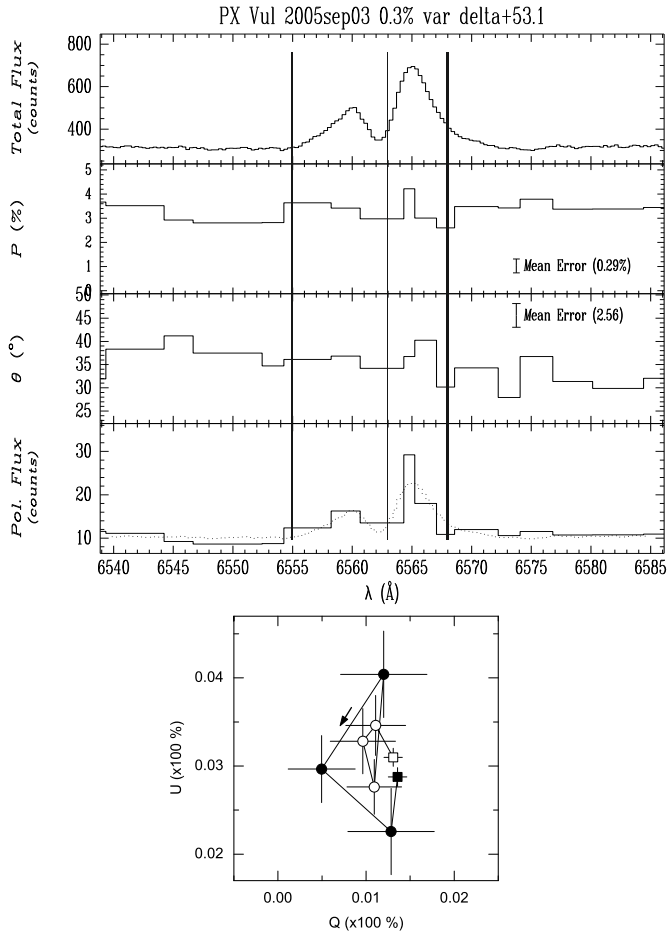

Fig. 4. Spectropolarimetry of PX Vul around Hα on 2005/Sep./03. *Top*: the huge vertical lines indicate the full region (6555−6568 Å) where the line effect is evident. The thin vertical line indicates the limit (6563 Å) between the blue and red line effect. The spectra are as in Fig. 2, binned using a variable bin size with a constant polarization error (per bin) of 0.3%. *Bottom*: $Q-U$ diagram showing the line effect (6555−6563 Å in white dots, 6563−6568 Å in black dots). The direction in which the wavelength increases is also indicated (arrow) along with the mean values for the blue (white square) and red (black square) continuum. The errors plotted around the line effect assume photon statistics directly.

computed by Petrov et al. (1999) is also shown. Analysing this diagram it seems clear that the solutions with $U' < 0$ for PA$_{int}$ are more likely. These solutions are indicated in the last column of Table 3. As we can see, the PA$_{int}$ values are practically the same (∼167°) between our two epochs considering the individual errors. As mentioned above, the same procedure applied by V03 to 2001 data yielded a PA$_{int}$ ∼ 146° (also shown in Fig. 3) that is consistent with our results within ∼20°. Therefore, the three existing measurements using the line effect in Hα spectropolarimetry yielded a mean PA$_{int}$ ∼ 160° with a variation range of ∼15°.

Assuming the ISP from Petrov et al. (1999) and discounting this value of the continuum polarization (Table 3), the intrinsic polarization is 1.6% at PA = 134° and 1.0% at PA = 149° in our 2004 and 2005 data, respectively. Vink et al. (2005a) reported continuum polarization around Hα in four epochs between 2001 and 2003. Therefore, considering the ISP used above, the mean intrinsic polarization for RY Tau between 2001 and 2005 is 1.3% at PA = 137°. The variation range of the PA$_{int}$ is ∼25° in this interval.

Comparing the mean values for the PA$_{int}$ by the above two methods, we obtained that they are reasonably consistent. In particular, the ISP corrected continuum method yields a PA$_{int}$ closer to perpendicular to the apparent disk direction (PA$_{disk}$ = 25°) derived from the jet (St-Onge & Bastien 2008). This fact reinforces the idea of an optically thin disk in RY Tau if single scattering is the prevailing mechanism. In addition, the apparent alignment between the disk direction and the ISP (see Fig. 3) suggests a weak interplay between the local magnetic field and its presumed collimator effect on the jet (De Colle & Raga 2005).

3.2. PX Vul

PX Vul (LHα 483-41) was initially cataloged as an early type star with a circumstellar shell and Hα in emission at a distance of 420 pc and belonging to the R association Vul R2 (Herbst et al. 1982). Its position is coincident with the edge of the filamentary cloud L778 near its northern NH_3 core (Myers et al. 1988). Mora et al. (2001) classified PX Vul as an early TTS (F3 Ve) and Hernandez et al. (2004) as a Herbig Ae/Be star (F3±1.5). Nevertheless, the last inferred masses ($\leq 2\ M_\odot$) by Eisner et al. (2005) and Manoj et al. (2006) seem more consistent with a TTS.

Optical photometric variability ($\Delta V \sim 0.3$ mag) was reported by Herbst et al. (1982). Nevertheless, Eiroa et al. (2002) classified PX Vul as non-variable ($\Delta V < 0.05$ mag). This object shows a moderate veiling level ($r_R = 0.8 \pm 0.4$), an important rotational velocity $v \sin i = 78 \pm 11$ km s^{-1}, and a higher mass-accretion rate of $1.3 \times 10^{-6}\ M_\odot\ \mathrm{yr}^{-1}$ (Eisner et al. 2005).

The optical polarization of PX Vul was not found to be variable by Oudmaijer et al. (2001). Their mean R broadband polarization (3.8% at PA = 27°) is comparable to our observed polarization integrated along the full spectrum (Table 3), therefore confirming the polarimetric non-variability.

The spectropolarimetry of PX Vul on 2005/Sep. is shown in Fig. 4. The total flux of Hα appeared as a double-peaked profile with the central dip at the continuum level. In relative fluxes,

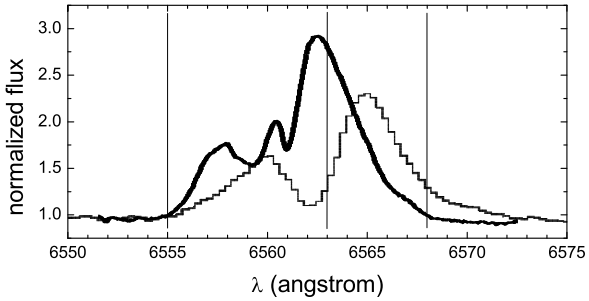

Fig. 5. Comparison of the Hα emission from PX Vul between 2004/Jun. (thick line, by Eisner et al. 2005 using Keck/HIRES) and 2005/Sep. (thin line, this work). The fluxes were normalized to the continuum in each case. The vertical lines are the same as in Fig. 4 to facilitate the comparison.

the red peak is ∼2.1 times more intense than the blue one. For comparison, Hα shows a triple-peaked profile on 2004/Jun. (Eisner et al. 2005) with the redder peak being more intense than the other two (1.8 and 3.9 times, respectively). The bluer peak is not present in our data (1.3 year after) and spectral variability seems to be present in the Hα emission changing from II−Bm to III−B type (Reipurth et al. 1996). This variability is also supported by the ratio between the redder peak and the continuum that falls from 2.9 (in 2004) to 2.3 (in 2005) (see Fig. 5).

As in Sect. 3.1, we detected the Hα polarization line effect for PX Vul using the $Q-U$ diagram. In this case, the main line effect is on the red peak (around three points in diagram between 6563−6568 Å) and appears as a loop consistent with the detection of a rotating disk. For a better comparison, we also plotted the points around the blue peak (6555−6563 Å) where another, subtle effect may be present. However, the strength of this effect is of the order of our errors and therefore this was not considered.

The linear fit to the points that display the loop in the $Q-U$ diagram yields two possible solutions for the PA_{int} (91 and 91 + 90°, Table 3). As previous information is not available, the ambiguity on PA_{int} cannot be solved for PX Vul. Following the sense of the PA rotation in the $Q-U$ diagram, the disk in PX Vul rotates in a counter-clockwise direction as seen from the Earth.

4. Summary and conclusions

We have shown here the first results of an ongoing spectropolarimetric survey of YSOs gathered with EIFU+IAGPOL at LNA. All the line detections shown in this work are significant at least in one of the Stokes parameters with a 95% confidence level.

The classical TTS RY Tau was observed in 2004 and 2005. Interestingly, the double-peaked Hα emission profile (II-B type) changed in ∼one year from a central dip at the continuum level to a dip just below the blue peak. RY Tau faded by about ∼0.8 mag between our observations with the blue/red peak ratio practically unchanged and without evidence of an anti-correlation between Hα and the photometry, as suggested by previous works.

Analysing the polarization spectra in the $Q-U$ diagram, RY Tau showed a well-defined line effect passing from a loop in 2004 to a more complex pattern (loop+linear excursion) in 2005. Our observations are consistent with previous spectropolarimetric data from V03 where loop detection was reported. This feature is interpreted as a signature of a compact source for Hα-line photons. The intrinsic polarization PA obtained directly from the line effect did not seem to change during our observations (PA_{int} ∼ 167°). We confirm that the disk in RY Tau rotates clockwise. Considering the continuum polarization, a slight enhancement was observed in 2005 with the PA practically unchanged (∼14°). The PA_{int} computed by the ISP corrected continuum method is more consistent with the presence of an optically thin disk in RY Tau.

For PX Vul, the comparison with previous spectra showed that spectral variability is present in the Hα emission passing from a II-Bm to II-B type in ∼1.3 yr. Nevertheless, the continuum polarization seems to be non-variable. We reported the detection of a rotating disk from the loop around Hα line in the $Q-U$ diagram. The intrinsic polarization has a PA ∼ 91° (with an ambiguity of 90°). An independent determination of the foreground polarization is necessary to better constrain the PA_{int}. The sense of the rotation of the PA on the loop shows that the direction of the disk rotation of PX Vul seems to be counterclockwise.

The finding of the signature of a loop in RY Tau and PX Vul confirms the trend of a compact source of line photons that is scattered off a rotating accretion disk in TTS.

Acknowledgements. A. P. thanks FAPESP (grant 02/12880−0) and CNPq (DTI grant 382.585/07−03 associated with the PCI/MCT/ON program). A.M.M. acknowledges support from FAPESP and CNPq. Polarimetry at IAG-USP is supported by FAPESP grant 01/12589−1.

References

Bailey, J., & Hough, J. H. 1982, PASP, 94, 618
Bastien, P. 1982, A&AS, 48, 153
Bastien, P., Drissen, L., Ménard, F., et al. 1988, AJ, 95, 900
Beck, T. L., & Simon, M. 2001, AJ, 122, 413
Bergner, Yu. K., Miroshnichenko, A. S., Yudin, R. V., et al. 1987, SvA Lett., 13, 84
Clarke, D., & McLean, I. S. 1974, MNRAS, 167, 27
De Colle, F., & Raga, A. C. 2005, MNRAS, 359, 164
Eiroa, C., Oudmaijer, R. D., Davies, J. K., et al. 2002, A&A, 384, 1038
Eisner, J. A., Hillenbrand, L. A., White, R. J., Akeson, R. L., & Sargent, A. I. 2005, ApJ, 623, 952
de Oliveira, A. C., et al. 2003, in Instrument Design and Performance for Optical/Infraed Ground-based Telescopes, ed. I. Masanori, & A. F. Moorwood (Bellingham: SPIE), Proc. SPIE, 4841, 1417
Henden, A. A. 2007, Observations from the AAVSO International Database, private communication
Herbst, W., Warner, J. W., Miller, D. P., & Herzog, A. 1982, AJ, 87, 98
Hernández, J., Calvet, N., Briceño, C., Hartmann, L., & Berlind, P. 2004, AJ, 127, 1682
Hough, J. H., Bailey, J., McCall, A., Axon, D. J., & Cunningham, E. C. 1981, MNRAS, 195, 429
Magalhães, A. M., Rodrigues, C. V., Margoniner, V. E., Pereyra, A., & Heathcote, S. 1996, ed. W. G. Roberge, & D. C. B. Whittet, ASP Conf. Ser., 97, 118
Manoj, P., Bhatt, H. C., Maheswar, G. & Muneer, S. 2006, ApJ, 653, 657
Ménard, F., & Bastien, P. 1992, AJ, 103, 564
Mora, A., Merín, B., Solano, E., et al. 2001, A&A, 378, 116
Myers, P. C., Heyer, M., Snell, R. L., & Goldsmith, P. F. 1988, ApJ, 324, 907
Oudmaijer, R. D., & Drew, J. E. 1999, MNRAS, 305, 166
Oudmaijer, R. D., Palacios, J., Eiroa, C., et al. 2001, A&A, 379, 564
Pereyra, A. 2000, Ph.D. Thesis, Instituto Astronômico e Geofísico, Universidade de São Paulo
Petrov, P. P., Zajtseva, G. V., Efimov, Yu. S., et al. 1999, A&A, 341, 553
Poeckert, R., & Marlborough, J. M. 1977, ApJ, 218, 220
Reipurth, B., Pedrosa, A., & Lago, M. T. V. T. 1996, A&AS, 120, 229
Schulte-Ladbeck, R., Clayton, G. C., Hillier, D. J., Harries, T. J., & Howarth, I. D. 1994, ApJ, 429, 846
Stassun, K., & Wood, K. 1999, ApJ, 510, 892
St-Onge, G., & Bastien, P. 2008, ApJ, 674, 1032
Tapia, S. 1988, Preprints of the Steward Observatory, 831
Vink, J. S., Drew, J. E., Harries, T. J., & Oudmaijer, R. D. 2002, MNRAS, 337, 356
Vink, J. S., Drew, J. E., Harries, T. J., Oudmaijer, R. D., & Unruh, Y. 2003, A&A, 406, 703, V03
Vink, J. S., Drew, J. E., Harries, T. J., Oudmaijer, R. D., & Unruh, Y. 2005a, MNRAS, 359, 1049
Vink, J. S., Harries, T. J., & Drew, J. E. 2005b, A&A, 430, 213
Vrba, F. J., Chugainov, P. F., Weaver, W. B., & Stauffer, J. S. 1993, AJ, 106, 1608
Wood, K., Brown, J. C., & Fox, G. K. 1993, A&A, 271, 492